Current Optics and Photonics
Vol. 2, No. 6, December 2018, pp. 589-594

ISSN: 2508-7266(Print) / ISSN: 2508-7274(Online)
DOI: https://doi.org/10.3807/COPP.2018.2.6.589

Two-dimensional Nature of Center-of-mass Excitons Confined in a Single CdMnTe/CdTe/CdMnTe Heterostructure

Woojin Lee[1†], Minwoo Kim[1†], Hanyi Yang[1], Kwangseuk Kyhm[1]*, Akihiro Murayama[2], Kuntheak Kheng[3], Henri Mariette[3], and Le Si Dang[4]

[1]Department of Cogno-Mechatronics Engineering, Physics Education, Pusan National University, Busan 46241, Republic of Korea
[2]Graduate School of Information Science and Technology, Hokkaido University, Sapporo 060-0814, Japan
[3]CEA, INAC-SP2M, Nanophysique et Semiconducteurs Group, F-38000 Grenoble, France
[4]Department of NANOscience, Institut Néel, CNRS, rue des Martyrs 38054, Grenoble, France

(Received November 11, 2018 : revised November 23, 2018 : accepted November 23, 2018)

We have investigated the dimensional nature of center-of-mass exciton confinement states in a CdMnTe/CdTe/CdMnTe heterostructure, where the CdTe well is too wide (144 nm) to confine both electrons and holes but able to confine whole excitons in the center-of-mass coordinate. Fine multiple photoluminescence spectra with a few meV separation were observed at 6 K. From the thickness dependence of the transition rate, they were attributed to even numbered center-of-mass exciton confinement states ($N = 2, 4, 6, \cdots, 18$). Dimensionality of the center-of-mass exciton confinement states was also investigated in terms of temperature dependence of radiative decay time. At low temperatures ($\lesssim$12 K), we found that the ground state excitons are likely localized possibly due to the barrier interface fluctuation, resulting in a constant decay time (~350 ps). With increased temperature ($\gtrsim$12 K), localized excitons are thermally released, giving rise to a linear temperature dependence of radiative decay time as an evidence of two-dimensional nature.

Keywords : Center-of-mass exciton, Radiative decay time, Dimensional nature, Excitation-correlation
OCIS codes : (160.6000) Semiconductor materials; (250.5230) Photoluminescence; (300.6500) Spectroscopy time-resolved

I. INTRODUCTION

In order to determine the dimensionality of semiconductor nanostructures, the confinement size (a) is compared with the exciton Bohr radius (a_B) as a criterion of the degree of confinement. For example, well layers with a thickness smaller than the exciton Bohr radius ($a < a_B$) are considered to be strongly confined, where the confined electrons and holes show a two-dimensional nature. On the other hand, as confinement size becomes larger than a_B, it is difficult to confine individual electrons and holes. In this case, excitons defined in the center-of-mass coordinate are confined as a single particle. These are known as center-of-mass exciton (CMX) confinement states. Because the total exciton mass is larger than the individual electrons and holes, the CMX confinement states are finely-spaced, within a few meV. In early work, the weakly confined CMX levels were observed in photoluminescence (PL), photoluminescence excitation (PLE), and reflectivity spectra [1-5].

While the thickness of two-dimensional quantum well structures ranges from a few nm up to several nm, an order-of-magnitude wider wells are used for the CMX confinement states. For example, the thickness of CdTe (50 nm and 100 nm) in CdTe/CdMnTe and CdTe/CdZnTe were far larger than the exciton Bohr radius of bulk CdTe ($a_B \sim 6$ nm). Although the CMX confinement states can be resolved spectrally, a large difference between the exciton

†These authors contributed equally to this work.
*Corresponding author: kskyhm@pusan.ac.kr, ORCID 0000-0003-3646-3560
Color versions of one or more of the figures in this paper are available online.

diameter and the confinement size brings into question whether the confined CMX can still be considered two-dimensional [1-5].

The confinement dimensionality can also be investigated in terms of a density of the states ($D(\varepsilon) \sim \varepsilon^{\beta}$), where the exponent β shows different characteristic values for three-dimensional (3D) bulk ($\beta = 0.5$), two-dimensional (2D) quantum wells ($\beta = 0$), and one-dimensional (1D) quantum wires ($\beta = -0.5$), respectively. When thermally excited excitons are relaxed along the exciton-polariton dispersion, temperature dependence of the radiative recombination rate is proportional to the population ratio of excitons near the bottleneck range with respect to the thermally distributed excitons. As the intra-relaxation of thermally distributed excitons is affected by the density of states, the confinement dimensionality gives rise to a temperature dependence of radiative recombination time ($\tau_r(T) \sim T^{\alpha}$). This method has been verified experimentally in 3D bulk ($\alpha \sim 1.5$), 2D quantum wells ($\alpha \sim 1$), and 1D quantum wires ($\alpha \sim 0.5$) [6-11]. However, time-resolved PL of the CMX confinement states has never been measured so far [12].

In this work, we have evaluated the confinement dimensionality of a CdTe/CdMnTe heterostructure in terms of temperature dependence of radiative recombination time ($\tau_r(T)$), where CMXs ($2a_B \sim 12$ nm) are weakly confined in a wide CdTe well ($a \sim 144$ nm). When the temperature is low ($\lesssim$12 K), we found that CMXs are likely localized possibly due to the interface fluctuation, resulting in a constant $\tau_r \sim 350$ ps. However, with increasing temperature, they show a linear temperature dependence ($\tau_r \sim T$). Therefore, the confined CMXs can still be considered a two-dimensional case.

II. METHODS

A single layer of CdMnTe/CdTe/CdMnTe heterostructure was grown by molecular beam epitaxy along the (100) direction. The structure was deposited on a ~4.2 μm $Cd_{0.9}Mn_{0.1}Te$ buffer layer, and the same Mn concentration was used for the barriers. The CdTe layer consists of 445 monolayers, and the thicknesses of ~144 nm was measured by reflection high energy electron diffraction (RHEED) oscillations [13]. Time-integrated PL and time-resolved PL were measured under excitation of ~100 femtosecond laser pulses, where the central wavelength was tuned near ~700 nm and repetition rate was 80 MHz. For a long-term time-resolved PL, we used streak camera system. For a relatively short-term decay of the intra-relaxation, we utilized an excitation-correlation technique. The sample was mounted in a temperature-controlled cryostat.

III. RESULTS AND DISCUSSION

As shown schematically in Fig. 1(a), the CMXs are weakly confined in a relatively large size (~10^2 nm), which is a range in between 3D bulk and 2D quantum well structures. Therefore, the CMX confinement states look quasi two-dimensional, and we used the terminology of heterostructures for the CMX confinement states instead of quantum wells. With a thin CdTe quantum well (<10 nm), the excitons shrink significantly along the confinement direction. On the other hand, in a thick CdTe layer (a = 144 nm), the exciton shrinkage looks minute compared to the size of spherical excitons in bulk ($2a_B \sim 12$ nm). Nevertheless, the wavelength of the CMXs are determined by finite CdTe well-size sandwiched between two potential barriers of $Cd_{0.9}Mn_{0.1}Te$. In thin 2D quantum well structures, separate confinements of electrons and holes should be considered. However, the CMXs are the case of a single particle confined in a wide potential well (Fig. 1(b)) [1-5].

Figure 1(c) shows PL spectrum at 4 K. PL peaks at 1591.5 meV and 1593 meV were known to be donor-bound excitons (D^0Xs) and charged excitons (X_c), respectively [14]. Along with a dominant PL peak near 1595 meV, several fine peaks are also seen with a few meV separation at the high energy spectrum up to 1602 meV. It is noticeable that the CMXs were excited within a potential well by using the tuned laser wavelength (~1.77 eV), whereby trapping of photo-induced carriers can be avoided near the well-barrier interface. Otherwise, the fine PL peaks of the CMX confinement states become blurred. Given potential well depth (~350 meV) and width (144 nm) of $Cd_{0.9}Mn_{0.1}Te$/CdTe/$Cd_{0.9}Mn_{0.1}Te$, the CMX confinement levels can be estimated. For the total mass ($M_X = m_e^* + m_{hh}^*$) of CMXs, the effective mass of the electron ($m_e^* = 0.088m_0$) and the heavy-hole mass ($m_{hh}^* = 0.60m_0$) were used with the electron rest mass m_0. The light-hole excitons 12.3 meV above the heavy-hole excitons are ignorable. Assuming that the wavefunction $\Psi_N(z)$ of the Nth-confined CMXs is zero for $|z|>a/2$, the even and odd symmetry form of $\Psi_N(z)$ are proportional to $cos(N\pi z/a)$ and $sin(N\pi z/a)$, respectively. However, the transition probability rate ($W = |C|^2|F_N(k_{ph})|^2$) also needs to be considered, where $|C|^2$ includes the dipole matrix element and the oscillator strength, and $F_N(k_{ph})$ is the Fourier-transformed function of $\Psi_N(z)$ at the photon wave vector near the exciton-polariton bottleneck (k_{ph}). For even and odd numbers of N, the Fourier components are given by,

$$F_N^2(k_{ph}) = \begin{cases} A_N^2 \cos^2(\frac{k_{ph}a}{2}) & \text{for } N = 1,3,5,\ldots, \\ A_N^2 \sin^2(\frac{k_{ph}a}{2}) & \text{for } N = 2,4,6,\ldots, \end{cases}, \quad (1)$$

$$A_N^2 = \frac{2}{a}\left[\frac{N\pi/a}{(N\pi/a)^2 - k_{ph}^2}\right]^2,$$

+whereby the decrease of PL intensity for N can also be explained [1-5].

In order to obtain k_{ph}, the CMX-polariton dispersion was calculated as shown in Fig. 1(d). Given the transverse frequency of excitons ($\omega_T = (E_g - E_X^b)/\hbar$) below the band gap ($E_g = 1.604$ eV) of CdTe with the exciton binding energy ($E_X^b = 10$ meV), a parabolic exciton dispersion can be described as $\omega_X(k) = \omega_T + \hbar^2k^2/2M_X$. Regarding light

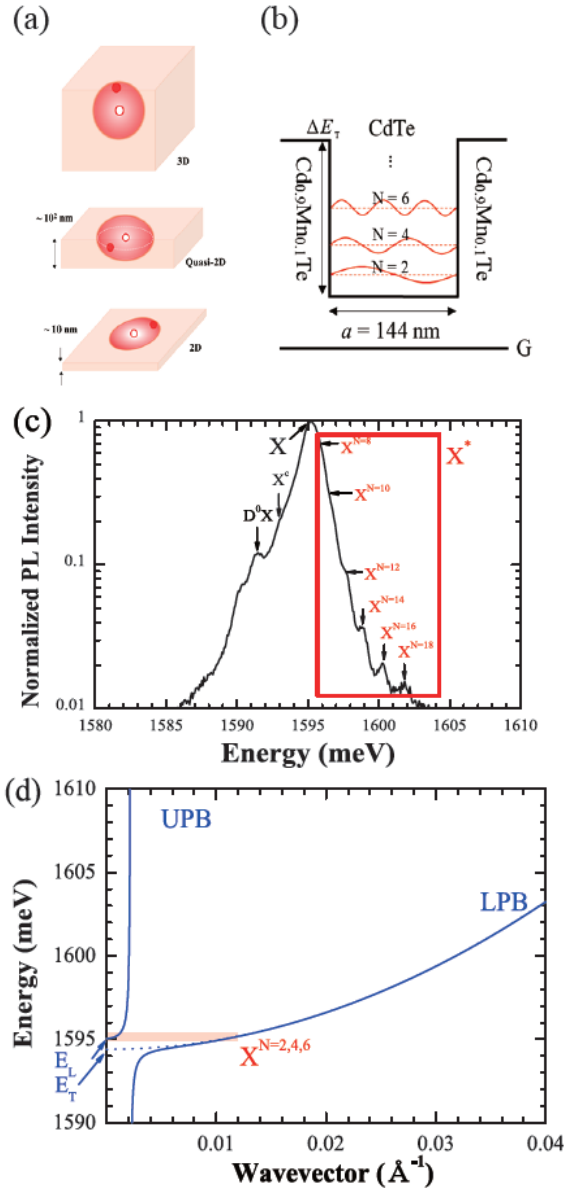

FIG. 1. (a) The center-of-mass excitons are weakly confined in an intermediate size (~10^2 nm) compared to strongly confined excitons of thin quantum wells (<10 nm) and unconfined excitons of bulk. (b) When a CdTe layer (a = 144 nm) is sandwiched between two $Cd_{0.9}Mn_{0.1}Te$ layers, only the even numbered CMX confinement states (N = 2, 4, 6, 8, 10, ⋯, 18) are dominant. (c) PL spectrum at 4 K. The dominant PL peak near 1595 meV is involved with three CMX confinement states (N = 2, 4, 6). (d) CMX-polariton dispersion.

dispersion with the electric permittivity $\epsilon_r(\omega)$, $k^2 = (\omega/c)^2\epsilon_r(\omega)$ becomes detailed according to the Lorentz model as

$$k^2 = \frac{\epsilon_b\omega^2}{c^2}\left[1 + \frac{f}{\omega_x^2 - \omega^2 - i\gamma\omega}\right], \quad (2)$$

where $\epsilon_b = 7.3$ is the background electric permittivity, and we ignored the damping coefficient $\gamma \simeq 0$ for simplicity. Given the longitudinal frequency $\omega_L = 2.42$ THz, we obtained the oscillator strength $f \simeq \omega_L^2 - \omega_T^2 \sim 4.78 \times 10^{27}\text{s}^{-2}$ [4, 5, 15-17]. As shown in Fig. 1(d), two branches of the CMX-polariton dispersion were obtained, where an anti-crossing of the linear light and the parabolic exciton dispersion appears near the longitudinal ($E_L = \hbar\omega_L$) and transverse energy ($E_T = \hbar\omega_T$). While the upper-polariton branch (UPB) shows a photon-like dispersion ($\hbar\omega = \hbar ck/\sqrt{\epsilon_b}$), the lower-polariton branch (LPB) is rather exciton-like ($\hbar\omega \sim \hbar^2k^2/2M_X$). It is noticeable that the transition probability rate W is determined while exciton-polaritons are relaxed along the stiff bottleneck of the LPB, where the wave vector of the LPB bottleneck (k_{ph}) is obtained. We found $k_{ph}a \simeq \pi$. Consequently, $F_N^2(k_{ph}) \simeq 0$ for the odd numbered states (N = 1, 3, 5, ⋯), and only the even numbered (N = 2, 4, 6, 8, ⋯, 18) states dominate. As shown in Fig. 1(d). We found that three (N = 2, 4, 6) CMX confinement states are involved in the dominant PL near 1595 meV, but the level separations are too small to resolve spectrally. Other excited fine levels in the PL spectrum were also identified up to N = 18 state. As N increases, the bottleneck energy becomes also increased. Nevertheless, the condition $k_{ph}a \simeq \pi$ still selects even numbered states for the excited states [3-5].

We have also investigated an intra-relaxation of the finely spaced CMX levels. While both streak camera and time-correlated single photon counting system are limited in time-resolution due to the instrumental response function (a few tens of ps), the excitation-correlation (EC) technique provides a population decay in a time scale of laser pulse duration (~100 fs) as shown schematically in Fig. 2(a). The first pulse gives rise to the population of electrons $n_e(t)$ and holes $n_h(t)$ of a certain confinement level at time t, and the second pulse with time delay τ generates $n_e(t+\tau)$ and $n_h(t+\tau)$. Therefore, each pulse generates time-integrated luminescence $\int n_e(t)n_h(t)dt$ and $\int n_e(t+\tau)n_h(t+\tau)dt$, respectively. However, τ-dependence of the EC signal results from the time-correlated luminescence $\int n_e(t)n_h(t+\tau)dt$ and $\int n_e(t+\tau)n_h(t)dt$, which is symmetric with respect to $\tau = 0$ as shown in Fig. 2(b). As the decay of the EC signal is fitted by ~ $\exp[-t/\tau_c]$, a characteristic time constant τ_c can be used as a measure of the CMX population decay. In Fig. 2(c), τ_c were obtained at the various CMX confinement levels in PL spectrum. In Fig. 2(d), the EC spectrum shows a redshift for increasing delay time (τ). Those results can be attributed to a consecutive intra-relaxation between the fine levels, whereby τ_c becomes decreased for the increased CMX confinement level [18-20].

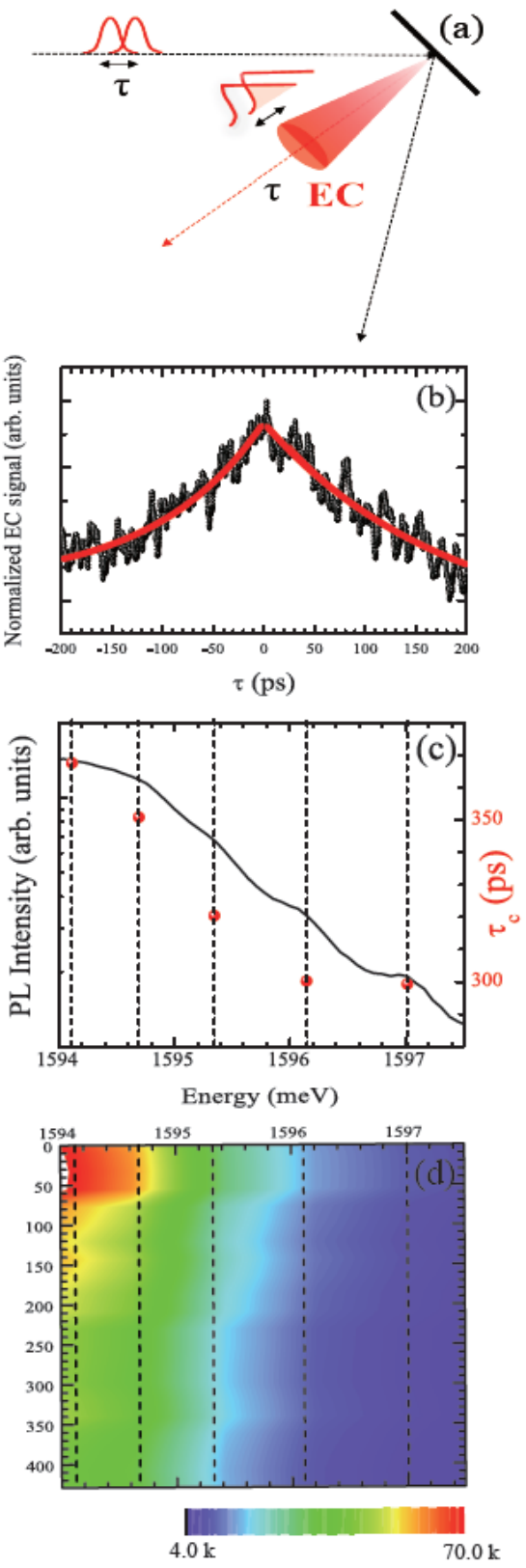

FIG. 2. (a) Schematic diagram of excitation-correlation (EC) spectroscopy, where excitation of a delayed pulse pair gives rise to correlated emission signals (b). (c) Characteristic decay time (τ_c) for the excited CMX states. (d) Spectral intensity of EC signals for delay time (τ).

Temperature dependence of the PL spectrum was also measured in Figs. 3(a), 3(b), and 3(c). By using two Gaussian functions, the resolution-limited three ($N = 2, 4, 6$) confinement states (X) and other ($N = 8, 10, \cdots, 18$) excited states (X^*) were fitted, whereby peak energy shift (ΔE_g) and linewidth broadening were obtained as a function of temperature. In Fig. 3(d), the temperature dependent peak energy shift (ΔE_g) of X and X^* were fitted by $\Delta E_g = -\alpha/[\exp(T_{ph}/T)-1]$, where the two fitting parameters α and T_{ph} correspond to the coupling strength of the phonon interaction and the Debye temperature, respectively. Additionally, the linewidth of X and X^* were found to increase linearly for increasing temperature up to 35 K as shown in Fig. 3(e). In this case, the linewidth broadening is dominated by acoustic phonon interactions, and temperature dependence of radiative decay time ($\tau_r(T)$) can be used to evaluate the confinement dimensionality [21, 22].

When excitons show a monotonic decay, the PL decay time (τ) is determined by radiative (τ_r) and non-radiative decay time (τ_{nr}), i.e. $1/\tau = 1/\tau_r + 1/\tau_{nr}$. In particular, the radiative transition rate of excitons ($1/\tau_r$) is determined in the photon-like bottleneck range ($k \lesssim 0.01 \text{Å}^{-1}$) in Fig. 1(d), where the transition strength ($F_X \sim 1/\tau_r$) is proportional to the oscillator strength and the wavefunction overlap of the electron with respect to the hole. As the exciton-acoustic phonon scattering becomes enhanced for increased temperature, the transitions need to be considered within a spectral width Δ. Therefore, the statistical fraction contributing to the radiative transition is given by

$$r(T) = \frac{\int_0^{\Delta} D(\varepsilon) e^{-\varepsilon/k_B T} d\varepsilon}{\int_0^{\infty} D(\varepsilon) e^{-\varepsilon/k_B T} d\varepsilon}, \tag{3}$$

where $D(\varepsilon) \sim \varepsilon^{\beta}$ is the exciton density of states for a given energy (ε), and the power factor β depends on the confinement dimensionality. As a result, the power factor α of temperature dependent radiative decay time ($\tau_r \sim T^{\alpha}$) can be utilized to evaluate the confinement dimensionality. While three-dimensional confinement gives rise to $\tau_r \sim T^{1.5}$ with $\beta = 0.5$, two-dimensional confinement shows a linear temperature dependence of the radiative decay time ($\tau_r \sim T$) with $\beta = 0$ [6-9]. Given the quantum efficiency $\eta = \tau_r^{-1}/\tau^{-1}$, radiative decay time ($\tau_r$) can be extracted from the PL decay time (τ). Because PL intensity is proportional to both excitation rate (g) and quantum efficiency, $I(T) = g\eta(T)$, PL intensity at a certain temperature $I(T)$ normalized to that at a reference temperature (6 K) can be used as a relative quantum efficiency $\zeta(T)$, i.e. $I(T)/I(6\text{ K}) = \eta(T)/\eta(6\text{ K}) = \zeta(T)$. As a result, temperature dependence of the radiative decay time can be obtained with a constant $\eta(6\text{ K})$ [23-25],

$$\tau_r(T)\eta(6\text{K}) = \frac{\tau(T)}{\zeta(T)}. \tag{4}$$

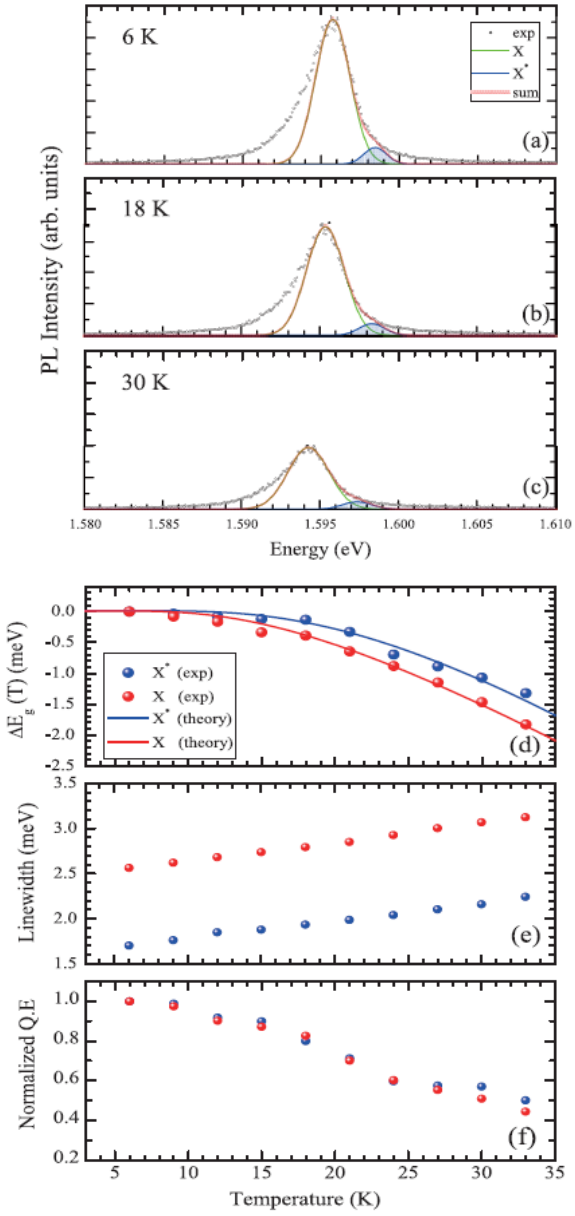

FIG. 3. Time-integrated PL spectrum at 6 K (a), 18 K (b), 30 K (c) are fitted with two Gaussian functions to analyze (American English) the resolution-limited three ($N = 2, 4, 6$) confinement states (X) and other ($N = 8, 10, \cdots, 18$) excited states (X^*), whereby temperature dependence of the central peak energy (d), linewidth (e), and normalized quantum efficiency (f) are obtained.

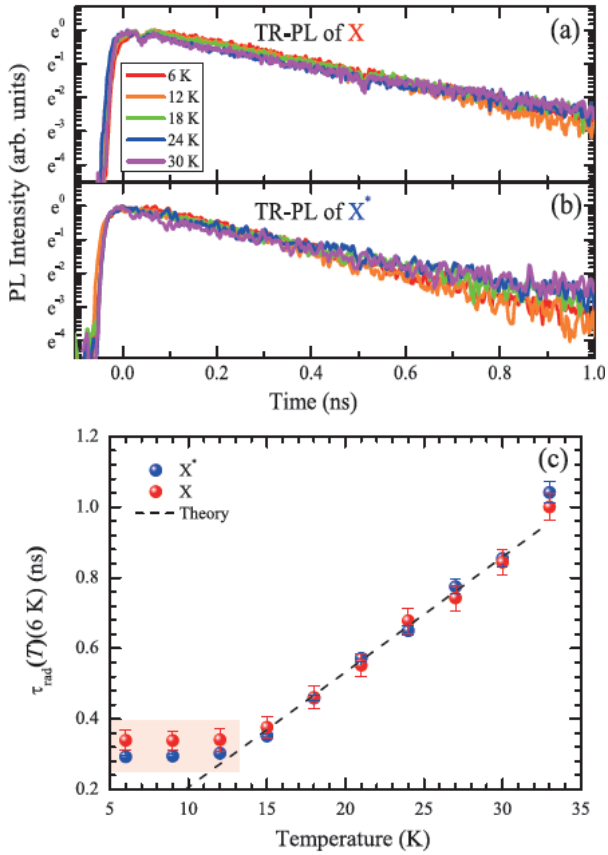

FIG. 4. Time-resolved PL intensity of X ($N = 2, 4, 6$) (a) and X^* ($N = 8, 10, \cdots, 18$) (b) were measured for increasing temperature, whereby temperature dependence of the radiative decay times (c) were also obtained. A theoretical model [28] (dotted line) of temperature dependent radiative recombination time (dotted line) was also compared, which suggest that the CMX confinement states show a two-dimensional nature when thermal energy is large enough ($\lesssim$12 K).

In Figures 4(a) and 4(b), both X and X^* show a monotonic PL decay for increasing temperature. By using Eq. (4), temperature dependence of the radiative decay time were also obtained for X and X^* in Fig. 4(c). When temperature is lower than 12 K, X and X^* show a constant radiative decay time of $\tau_r \sim 350$ ps. This can be attributed to weak localization at the interface fluctuation, which are likely observed in II-VI heterostructures [26, 27]. However, as temperature is increased over 12 K, a linear temperature dependence ($\tau_r \sim T$) is observed as an evidence of the two-dimensional nature [6, 7, 27]. The linear temperature dependence in two-dimensional confinement structures is given by $\tau_r(T) = 3M_X k_B T\tau_0/\hbar^2 k_0^2$. As heavy-holes are dominant [28, 29], we found the intrinsic radiative lifetime $\tau_0 \sim 45$ ps from the linear slope (~32 ps/K).

IV. CONCLUSION

When a thick (144 nm) CdTe layer is confined by CdMnTe, which is far large compared to the exciton-Bohr radius ($a_B \sim 6$ nm), we found that the weakly confined center-of-mass confinement states show a linear temperature dependence of the radiative decay time as an evidence of the two-dimensional nature. Although the excitons are likely localized at low temperature (<12 K), the weakly confined center-of-mass excitons can be considered as a two-dimensional case for increased temperature up to 35 K.

ACKNOWLEDGEMENT

This work was supported by a 2-Year Research Grant of Pusan National University.

REFERENCES

1. H. Mariette, N. Magnea, and H. Tuffigo, "Optical investigation of CdTe/CdZnTe Heterostructures," Phys. Scripta **T39**, 204-210 (1991).
2. H. Tuffigo, B. Lavigne, R. T. Cox, G. Lentz, and N. Magnea, "Strong effects of electron-hole Coulomb interaction on optical properties of CdTe quantum wells," Surf. Sci. **229**, 480-483 (1990).
3. Y. M. d'Aubigné, L. S. Dang, A. Wasiela, N. Magnea, F. d'Albo, and A. Million, "Quantization of excitonic polaritons in CdTe-CdZnTe double heterostructures," J. Phys. Colloques **48**, C5-363-C5-366 (1987).
4. H. Tuffigo, R. T. Cox, G. Lentz, and N. Magnea, "Optical properties of excitons in II-VI quantum wells: importance of centre-of-mass quantization," J. Cry. Grow. **101**, 778-782 (1990).
5. H. Tuffigo, R. T. Cox, N. Magnea, Y. M. d'Aubigné, and A. Million, "Luminescence from quantized exciton-polariton states in $Cd_{1-x}Zn_xTe/CdTe/Cd_{1-x}Zn_xTe$ thin-layer heterostructures," Phys. Rev. B **37**, 4310-4313 (1988).
6. J. Feldmann, G. Peter, E. O. Göbel, P. Dawson, K. Moore, C. Foxon, and R. J. Elliott, "Linewidth dependence of radiative exciton lifetimes in quantum wells," Phys. Rev. Lett. **59**, 2337-2340 (1987).
7. H. Akiyama, S. Koshiba, T. Someya, K. Wada, H. Noge, Y. Nakamura, T. Inoshita, and A. Shimizu, "Thermalization effect on radiative decay of excitons in quantum wires," Phys. Rev. Lett. **72**, 924-927 (1994).
8. H. Kim, W. Lee, S. Park, K. Kyhm, K. Je, R. A. Taylor, G. Nogues, L. S. Dang, and J. D. Song, "Quasi-one-dimensional density of states in a single quantum ring," Sci. Rep. **7**, 40026 (2017).
9. W. Lee, T. Kiba, A. Murayama, C. Sartel, V. Sallet, I. Kim, R. A. Taylor, Y. D. Jho, and K. Kyhm, "Temperature dependence of the radiative recombination time in ZnO nanorods under an external magnetic field of 6T," Opt. Express **22**, 17959-17967 (2014).
10. S. Chen, M. Yoshita, A. Ishikawa, T. Mochizuki, S. Maruyama, H. Akiyama, Y. Hayamizu, L. N. Pfeiffer, and K. W. West, "Intrinsic radiative lifetime derived via absorption cross section of one-dimensional excitons," Sci. Rep. **3**, 1941 (2013).
11. G. W. p't Hooft, W. A. J. A. van der Poel, L. W. Molenkamp, and C. T. Foxon, "Giant oscillator strength of the excitons in GaAs," Phys. Rev. B **35**, 8281-8284 (1987).
12. H. P. Wagner, A. Scha¨tz, R. Maier, W. Langbein, and J. M. Hvam, "Interaction and dephasing of center-of-mass quantized excitons in wide $ZnSe/Zn_{0.94}Mg_{0.06}Se$ quantum wells," Phys. Rev. B **57**, 1791-1796 (1998).
13. I. Lawrence, G. Feuillet, H. Tuffigo, C. Bodin, J. Cibert, and W. W. Rühle, "Optical study of an asymmetric double quantum well system: CdTe/CdMnTe," Acta Phys. Pol. A **84**, 637-640 (1993).
14. K. Kheng, R. T. Cox, Y. M. d'Aubigné, F. Bassani, K. Saminadayar, and S. Tatarenko, "Observation of negatively charged excitons X^- in semiconductor quantum wells," Phys. Rev. Lett. **71**, 1752-1755 (1993).
15. O. Zakharov, A. Rubio, X. Blase, M. L. Cohen, and S. G. Louie, "Quasiparticle band structures of six II-VI compounds: ZnS, ZnSe, ZnTe, CdS, CdSe, and CdTe," Phys. Rev. B **50**, 10780-10787 (1994).
16. H.-z. Wu, A.-l. Yang, J.-z. Wu, Z.-z. Li, "Exciton properties of diluted CdTe/CdMnTe quantum wells," Chin. Phys. Lett. **15**, 734-736 (1998).
17. J. J. Hoffield and D. G. Thomas, "Theoretical and experimental effects of spatial dispersion on the optical properties of crystals," Phys. Rev. **132**, 563-572 (1963).
18. D. von der Linde, J. Kuhl, and E. Rosengart, "Picosecond correlation effects in the hot luminescence of GaAs," J. Lum. **24/25**, 675-678 (1981).
19. A. M. de Paula, R. A. Taylor, C. W. W. Bradley, A. J. Turberfield, and J. F. Ryan, "Investigation of inter-valley scattering and hot phonon dynamics in GaAs quantum wells using femtosecond luminescence intensity correlation," Superlattice. Microst. **6**, 199-202 (1989).
20. R. Mondal, B. Bansal, A. Mandal, S. Chakrabarti, and B. Pal, "Pauli blocking dynamics in optically excited quantum dots: A picosecond excitation-correlation spectroscopic study," Phys. Rev. B **87**, 115317 (2013).
21. L. Besombes, K. Kheng, L. Marsal, and H. Mariette, "Acoustic phonon broadening mechanism in single quantum dot emission," Phys. Rev. B **63**, 155307 (2001).
22. L. C. Andreani, A. d'Andrea, and R. del Sole, "Excitons in confined systems: from quantum well to bulk behaviour," Phys. Lett. A **168**, 451-459 (1992).
23. R. C. Miller, D. A. Kleinman, W. A. Nordland, Jr., and A. C. Gossard, "Luminescence studies of optically pumped quantum wells in $GaAs\text{-}Al_xGa_{1-x}As$ multilayer structures," Phys. Rev. B **22**, 863-871 (1980).
24. D. Takamizu, Y. Nishimoto, S. Akasaka, H. Yuji, K. Tamura, K. Nakahara, T. Onuma, T. Tanabe, H. Takasu, M. Kawasaki, and S. F. Chichibu, "Direct correlation between the internal quantum efficiency and photoluminescence lifetime in undoped ZnO epilayers grown on Zn-polar ZnO substrates by plasma-assisted molecular beam epitaxy," J. Appl. Phys. **103**, 063502 (2008).
25. C. H. Ahn, S. K. Mohanta, N. E. Lee, and H. K. Cho, "Enhanced exciton-phonon interactions in photoluminescence of ZnO nanopencils," Appl. Phys. Lett. **94**, 261904 (2009).
26. M. Lomascolo, P. Ciccarese, R. Cingolani, R. Rinaldi, and F. K. Reinhart, "Free versus localized exciton in GaAs V-shaped quantum wires," J. Appl. Phys. **83**, 302-305 (1998).
27. M. Colocci, M. Gurioli, and J. Martinez-Pastor, "Exciton relaxation dynamics in quantum well heterostructures," Le J. Phys. IV **3**, C5-3-C5-10 (1993).
28. L. C. Andreani, "Radiative lifetime of free excitons in quantum wells," Solid State Commun. **77**, 641-645 (1991).
29. N. Magnea, F. Dal'bo, C. Fontaine, A. Million, J. P. Gaillard, L. S. Dang, Y. M. d'Aubigné, and S. Tatarenko, "Mismatch strain measurements of MBE grown CdTe," J. Cry. Grow. **81**, 501-504 (1987).